Tsunami arrival time characteristics of the 2011 East Japan Tsunami obtained from eyewitness accounts, evidence and numerical simulation

Abdul Muhari*
Fumihiko Imamura*
Anawat Suppasri**
Erick Mas*

*Tsunami Engineering Lab
International Research Institute for Disaster Science (IRIDeS), TOHOKU University
**Endowed Research Division
International Research Institute for Disaster Science (IRIDeS), TOHOKU University

ABSTRACT

Information on the tsunami arrival time for people located along a coastline is crucial for community-based tsunami preparedness activities. It is also important for tsunami source mechanism studies to support other field observation data such as run-up heights, co-seismic subsidence and eyewitness accounts. In this study, we reconstructed the tsunami arrival times along the east coast of Japan during the 2011 tsunami. As most of the tide gauges were damaged, first we collected and analyzed the arrival time data from equipment that survived the tsunami. The tsunami waveforms offshore were taken from six GPS buoys covering the Fukushima coastline in the south to Aomori in the north. Next, we utilized the records from stopped clocks found in the tsunami affected areas to briefly view the inundation arrival time. In addition to the observed run-up data, we used the above-mentioned arrival time information to propose and validate a new source mechanism for the 2011 Japan tsunami. The well-validated source model was then used to obtain the characteristics of the tsunami arrival time along the east coast of Japan. The results can be used as primary information for designing a community-based evacuation plan and increasing community awareness of tsunamis.

Keyword: tsunami arrival time, near-field, eyewitness and evidence

1 Introduction

1.1 Background

In tsunami-prone areas, the evacuation of residents is generally expected to be triggered by the official warning system. However, in many cases it is the natural warning i.e., the receding wave at the shoreline, that influences the evacuee's decision. Despite the availability of a tsunami early warning system, some people still went to the beach to see whether a low tide had occurred (I-RAPID, 2012, Hoppe and Mahadiko, 2010). As stated by Sorensen (1991) people appear to adjust their reaction to the timing of an impending threat (Mas E., 2012). Based on that idea, it is important to address the arrival time of a tsunami and the characteristics of its initial waveform, such as

the positive and negative initial wave. By doing so, it is possible to show that a leading negative wave may not precede the tsunami even in the near-field case. Such information is probably not that important for people with a tsunami early warning system as advanced as that in Japan. However, it could provide a very important lesson to be shared with communities in areas where tsunami early warning systems are not fully functional. Nevertheless, such information can also be used for community-based tsunami preparedness along the east coast of Japan.

In contrast, tsunami arrival time information is essential for the study of the tsunami source mechanisms. Satake and Kanamori (1991) proposed the inverse theory to study earthquake sources based on tsunami waveforms in the tide gauges. Shuto and Matsutomi (1995), and Takahashi et al. (1995) stressed the necessity of arrival time from eyewitness accounts to develop the tsunami source in a forward modeling framework. However, in the case of the 2011 Japan tsunami, most of the tide gauges were destroyed so only very limited data can be used. Relying on the available waveforms data of GPS buoys (MLIT, 2011) sometimes cannot reproduce the observed run-up data since the gauge wave heights do not necessarily correlate with the heights of tsunami run-ups in the vicinity of the gauge (Titov et al., 2005). Results demonstrated by MacInnes et al. (in press) clearly show such discrepancy. Their results of the modeled tsunami run-ups from nine different source models differ significantly from the observed data. In this study, therefore, we utilized information of two different arrival times to support the source modeling study. The tsunami waveforms of GPS buoys data were complemented by the inundation arrival time from the stopped clocks to fill the blanks due to the lack of information from the tide gauges along the coast. In addition to the observed run-up heights data, the tsunami source model for the 2011 tsunami was proposed and validated using the above-mentioned arrival time data. The well-validated source model was then used to reveal the characteristics of tsunami arrival times along the east coast of Japan during the 2011 tsunami.

1.2 Outline of the paper

This paper is organized as follows. First, the arrival time is described and interpreted based on tsuna-

mi waveforms of six GPS buoys and from the stopped clocks in the tsunami affected areas. In the next section, we examine the source model of Tohoku University version 1.1 (e.g., Sugawara et al., 2011) in accordance with both arrival time data and the observed run-up heights by Mori et al. (2012). Based on the results of the examination, we propose an enhanced source model to reproduce the observational data. Finally, the tsunami arrival time along the east coast of Japan is reconstructed using the well-validated source model and summarized in a simple representation.

2 Description of the arrival time data

2.1 Field evidence and eyewitness accounts

Information about the tsunami arrival time was collected from intensive research of newspapers, Internet blogs and other private addresses, interviews, books and magazines in addition to our documentation and photographs taken during the frequent post-tsunami surveys. The database consists of seventy-nine stopped clocks and eyewitness accounts. Original information including the address of Internet sources is provided in the supplement to this paper. We searched the coordinates of those data through the satellite image analysis and ground checked during the field survey, which are spatially distributed from Fukushima to Aomori Prefecture (Fig. 1). Particularly for the clocks data, determining the tsunami arrival time from stopped clocks might be controversial due to the possibility of human intervention in the swept away clocks (e.g., Lavigne et al., 2009). In this study, therefore, we selected only clocks that had been placed on relatively high walls to ensure that they were out of human reach. The other consideration is that the clocks might have stopped in the range of the first initial tsunami arrival up to the first peak of the tsunami wave. Thus, validation of the modeled tsunami using the clocks data should take this into account. The arrival time data plotted in Fig. 1 gives the general impression that the tsunami arrival time ranged from 25 to 55 min except in the area of Sendai Bay. The trend line of the data shows that the tsunami arrival time might be correlated with the beach's strike relative to the fault's strike (trench line) in north Iwate to Aomori. Down to the south, the arrival time in south Sanriku and the Sendai Plain might be correlated with the distance of the places relative to the
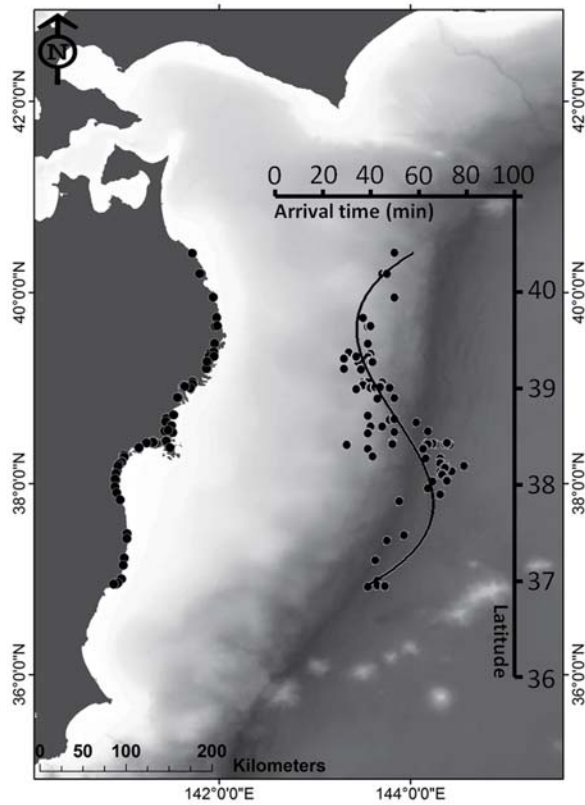
Figure1. Tsunami arrival times from eyewitness accounts and stopped clocks.

source area, and some local effect such as shoaling due to shallow water in the bay region.

More detailed descriptions of the stopped clocks data and their possible correlation with the tsunami source are given in the following sub-sections.

2.1.1 Aomori, Sanriku coast of Iwate and North Miyagi

The beach's strike of north Iwate to Aomori Prefecture is opposite to that of the fault's strike. The arrival time toward the north, therefore, lengthens compared to the southward region. Here, the arrival time ranges from 40 min in Miyako and Taro to 50 min in Hashikami. From the middle of Iwate to the south up to the northern part of Miyagi Prefecture, the so-called Sanriku coast is characterized by ria coastline, which might influence the arrival time particularly in cities inside a long V-shaped bay. This region may be close to the earthquake source area because the arrival time ranges only from 25 to 40 min. A photograph of a stopped clock in a damaged building taken in Taro town of Miyako City shows that the tsunami inundated the area 40 min after the earthquake. A similar indication was observed from stopped clocks at Otsuchi Town Hall (40 min). Moving further south, the stopped clock in Kamaishi-Higashi Junior High School was at the 39 min arrival time mark as well as in street clocks at Ofunato. However, starting from Rikuzentakata toward the south, the tsunami arrival time increased as indicated by a clock found in Rikuzentakata Dai-Ichi Junior High School that stopped 44 min after the earthquake. Another photograph of a stopped clock taken near a fish market in Kesennuma and in the disaster prevention building at Minami-Sanriku shows tsunami arrival times of 50 min and 48 min, respectively. Moreover, stopped clocks in Onagawa Hospital and Ookawa Elementary School (Fig. 2, left) in north Ishinomaki show that the tsunami had a similar arrival time ranging from 49 and 50 min,

Figure2. Stopped clocks at Ookawa elementary school, Ishinomaki (left), Sendai port (center), and Kaisei high school (right)

respectively. Based on the above-mentioned data, preliminary hypotheses suggest that the earthquake source may be close to the shore in the region from Miyako to the south up to the vicinity of Oshika Peninsula (near Onagawa and Ishinomaki City).

2.1.2 Sendai Plain to the south in north Fukushima

Sendai and Ishinomaki City are plain areas located inside Sendai bay, which is characterized by shallow water depth. In accordance with shoaling phenomenon, the tsunami arrived in these areas with a comparatively slower arrival time of about 60 to 70 min. In Ishinomaki City, a stopped clock at Ishinomaki Girls Commercial High School shows that the tsunami arrived 73 min after the earthquake. In Higashi-Matsushima Naruse Dai-Ni Junior High School, tsunami inundation arrived in 62 min. Further to the south of the Sendai Plain, stopped clocks in Sendai Port (Fig. 2, center), Arahama Elementary School and Coastal Adventure Park showed that the tsunami arrival time was 69 min, 69 min and 71 min, respectively.

In the area close to Sendai Airport, the tsunami arrival time in Natori City was estimated as 71 min from the stopped clock in Yuriage Elementary School. Also, clocks at Sendai Airport terminal indicated that the tsunami arrived 74 min after the earthquake. A relatively similar arrival time was also observed at Iwanuma and in a hot spa at Watari, which accordingly stopped at 70 min as interpreted from a photograph of the tsunami arriving at Tenzanbori Channel, and 66 min as visualized from a helicopter and photograph taken by an eyewitness.

2.1.3 Fukushima coast

The Fukushima coast connects with the southern part of the Sendai Plain. Thus, the tsunami arrival time in this area is relatively similar to that of the Sendai Plain (60 to 70 min). This is confirmed by stopped clocks in a fisheries cooperative in Shinchi (64 min) and in central Soma (69 min). However, toward the south in central and southern Fukushima, the coasts were no longer influenced by the shallow water in Sendai bay; thus, the tsunami arrival time increased in speed as observed at about 40 to 50 min confirmed by a stopped clock in Ukedo School at Namie town (52 min), Fukushima Dai-Ichi Nuclear Power Plant (54

min), Takano Hospital in Futaba district (47 min) and in Kaisei High Schools in Iwaki (39 to 43 min, Fig. 2, right).

2.2 Tide gauges and tsunami run-up data

In the near-field case, local variation of the tsunami was highly dependent on the slip distribution (e.g., Geist and Dmowska, 1999). To interpret the arrival time from six GPS buoys installed along the east coast of Honshu Island (MLIT, 2011), we used definitions given by Hayashi et al. (2011). They divided arrival time into four major components namely the tsunami arrival time, initial trough, local crest and primary crest.

Interpretation derived from the GPS buoys data can be summarized in several hypotheses. First, the sudden drop in water level that occurred just after the earthquake in GPS 801, 802, 803 and 804 (Sendai, Sendai north, Iwate south, and Iwate) indicated that they were placed inside the earthquake source area. The local crests in Fukushima (GPS 806) and Iwate (GPS 804) suggest that a minor fault exists in addition to the major fault (e.g., Shuto and Matsutomi,
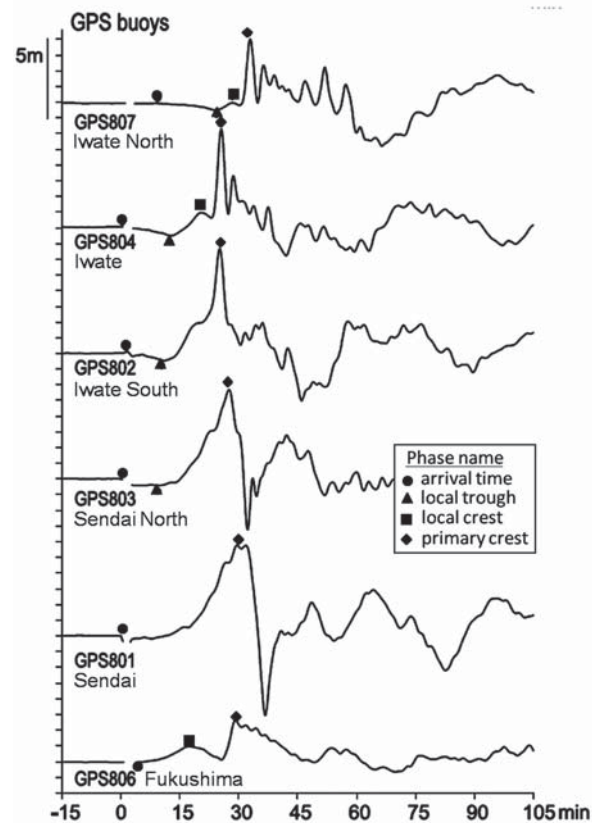
Figure3. Descriptions of tsunami arrival time according to Hayashi et al. (2011)

1995). In GPS 802, 803 and 804 the primary crest has a small period that indicates the major slip may be accompanied by additional uplift in the shallow sediment (e.g., Tanioka and Seno, 2001) or indicates complex rupture involving reverse and normal faults (Tsuji et al., 2011a). In the northernmost area, GPS 807 has a delay in its arrival time as well as primary crest that indicate this buoy may be placed in the area farthest from the major fault.

3 Numerical analysis

3.1 Developing tsunami source mechanism

To date, many source generation models of the 2011 Tohoku Tsunami have been proposed from a seismological perspective. Huge amounts of land- and ocean-based geophysical equipment provide the prospect of disclosing the mega-thrust phenomenon for better understanding of large earthquake generation. However, to date almost none of the developed earthquake sources have been able to reproduce the tsunami run-up data. Regarding the latter, Maeda et al. (2011) reconstructed two stages of the observed tsunami wave at an ocean bottom tsunami sensor placed in Kamaishi. Fujii et al. (2011) estimated the slip distribution from the tsunami inversion in several tide gauges. But these two source models proved unable to reproduce the observed run-up data. Yamazaki et al. (2011) used an earthquake source from seismic and geodetic observation (Lay et al., 2011 and Yue and Lay, 2011) for near-field tsunami modeling. However, their efforts are limited to only the validation us-

ing the GPS buoys and the available tide gauges data. Recently, MacInnes et al. (in press) compared the resulting modeled tsunami from nine different source models based on seismic inversion, tsunami waveforms and GPS data. As a result, some of them can perfectly reproduce the tsunami waveforms at several DART buoys; none of them are able to reproduce the run-up data, not even the trend.

Apart from the seismic and tsunami waveforms data, Tohoku University developed the source mechanism (DCRC, 2011) by stressing the reconstruction of the observed run-up and inundation data (JSCE, 2011). The result from inundation modeling using SRTM data with a cell size of 90 is given in Fig. 4. It shows that the pattern of the observed run-up data is reproduced except in the area where the highest run-up was recorded. According to the data presented by Tsuji et al. (2011b), most of those highest run-ups were observed around the hills with very steep slope topography. A similar situation was observed during the 1993 Okushiri Tsunami in Monai (Shuto and Matsutomi, 1995) and the 2010 Chile Tsunami in Constitution (Imamura et al., 2010). With the present numerical grid size, it is impossible to reproduce those types of run-up heights. Shuto and Matsutomi (1995) suggest that a finer grid of less than 5 m is required to reproduce that very high run-up data. More detailed verification of the proposed source model for the observed run-up data can be found in DCRC (2012).

However, the proposed source model has unsatisfactory agreement when compared to the data from the GPS buoys as seen in Fig. 5. To overcome the
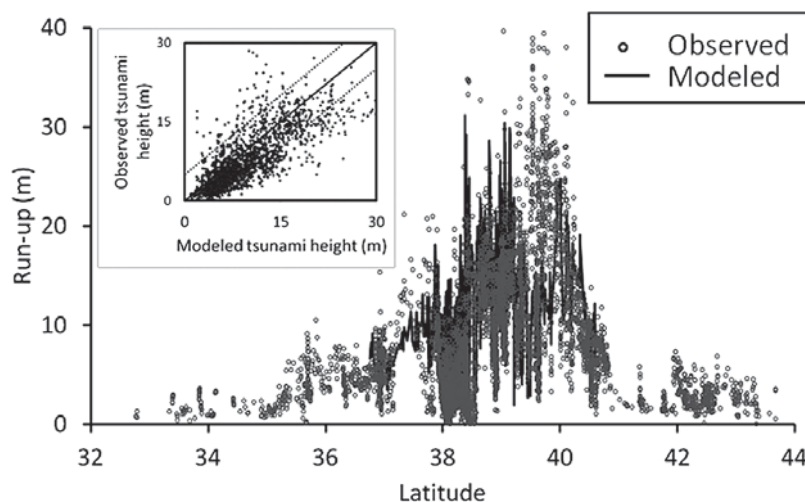

Figure4. Comparison of modeled run-up heights based on Tohoku Univ. 1.1 model with the observed data

discrepancy with the waveforms data, we adopted a traditional forward modeling approach with trial and error method to enhance this source model without significantly reducing the accuracy that was obtained against the run-up.

Based on the source model provided by Tohoku University version 1.1, we divided the rupture area into eleven regions with length and width that vary from 25 to 175 km (Fig. 6 left). The slip values vary from 1 to a maximum of 50 m near the trench (Table 1). This configuration gives a resulting moment magnitude M_0 of 4.1×10^{22} N m, yield to a 9.0 Mw earthquake assuming a homogenous rigidity of 5.0×10^{10}

N/m^2. As also indicated by Maeda et al. (2011) and Fujii et al. (2011), large uplift exists near the trench with a shorter period to reproduce the two stages of tsunami observed in GPS buoys at Iwate Prefecture.

The resulting sea-floor displacement calculated using a static deformation model (Okada, 1985) gives a maximum vertical uplift near the trench of 22.7 m, and a maximum subsidence of 1.8 m observed at nearby Oshika peninsula (Fig. 6, right). In the latter, the value obtained from the source model is slightly higher than the subsidence of 1.2 m observed by the Geospatial Survey Institute of Japan (GSI, 2011).
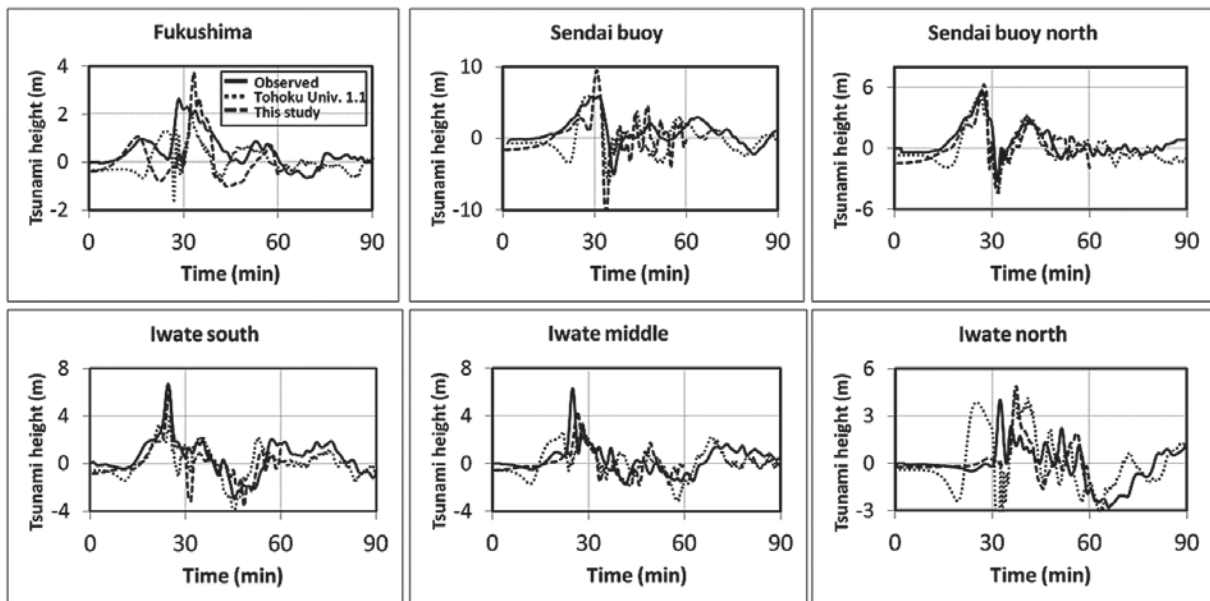
Figure5. Comparison of the observed tsunami waveforms with the modeled tsunami based on the source model of Tohoku Univ. 1.1 and source model proposed by this study

Table1. Description of the proposed source model

No	Length (km)	Width (km)	X	Y	slip (m)	depth (m)	dip	strike	rake
1	100000	100000	144.200	39.300	5.00	1000	14	193	81
2	100000	50000	143.939	38.424	50.00	1000	14	193	81
3	100000	50000	143.397	38.552	30.00	12000	14	193	81
4	100000	100000	143.682	37.547	7.50	1000	14	193	81
5	100000	125000	143.070	36.730	1.00	1000	14	193	81
6	100000	175000	144.258	40.239	1.00	24000	14	193	81
7	100000	75000	143.100	39.496	3.00	24000	14	193	81
8	100000	50000	142.853	38.620	20.00	24000	14	193	81
9	100000	50000	142.309	38.718	10.00	36000	14	193	81
10	100000	100000	142.609	37.744	2.00	24000	14	193	81
11	100000	75000	141.800	37.004	10.00	36000	14	193	81

3.2 Validation of the proposed source model

We modeled the tsunami propagation in two domains constructed in a nested grid system (Fig. 6, right). Data of GEBCO_08 (British Oceanographic Data Center, 2008) was resampled into a cell size of 270 m and used in Region 1. For Region 2, we used data of the Shuttle Radar Topographic Mission (SRTM, CGIAR-CSI) and retained the original accuracy of 90 m as the cell size.

Reliability of the source was examined using the Aida K and κ, which is the geometric mean of the ratio of the measured amplitude, period and run-up heights to that of those computed, while κ is the corresponding standard deviation (Aida, 1978). Also, the Root Mean Square Error/Deviation was used in the evaluation.

$$\log K = \frac{1}{n} \sum_{i=1}^{n} \log K_i \qquad K_i = \frac{R_i}{H_i}$$

$$\log \kappa = \sqrt{\frac{1}{n} \sum_{i=1}^{n} (\log K_i)^2 - (\log K)^2} \qquad (1)$$

$$\text{RMSD} = \sqrt{\frac{\sum_{i=1}^{n} (x_{1,i} - x_{2,i})^2}{n}}. \qquad (2)$$

Shuto (1991) suggests values of $0.8 < K < 1.2$ and $\kappa < 1.45$, while the Japan Society of Civil Engineers suggests values of $0.95 < K < 1.05$ and $\kappa < 1.45$ to judge the initial profile as satisfactory (JSCE, 2006).

We used linear long wave theory in Region 1 and non-linear shallow water theory in Region 2, which is solved using the finite difference method on a staggered leap frog scheme (Imamura, 1996). The total time of simulation was 1.5 hours with increments of 0.5 sec for Region 1 and 0.15 sec for Region 2, respectively. The manning coefficient used in Region 2 was similar for the entire domain as 0.025.

We first validated the proposed source model for the tsunami waveforms at six GPS buoys as given in Fig. 5. Here, *a1* means the first peak (which can be the local or primary crest) and *a2* is the first drop that is the initial trough. It is shown that the proposed source model can perfectly reproduce two stages of the tsunami wave in Iwate south. Also, it can reduce the leading negative wave that produced the previous result. A comparison of the Tohoku Univ. 1.1 model with the present study given in Table 2 demonstrates a significant improvement in the reliability indicated by
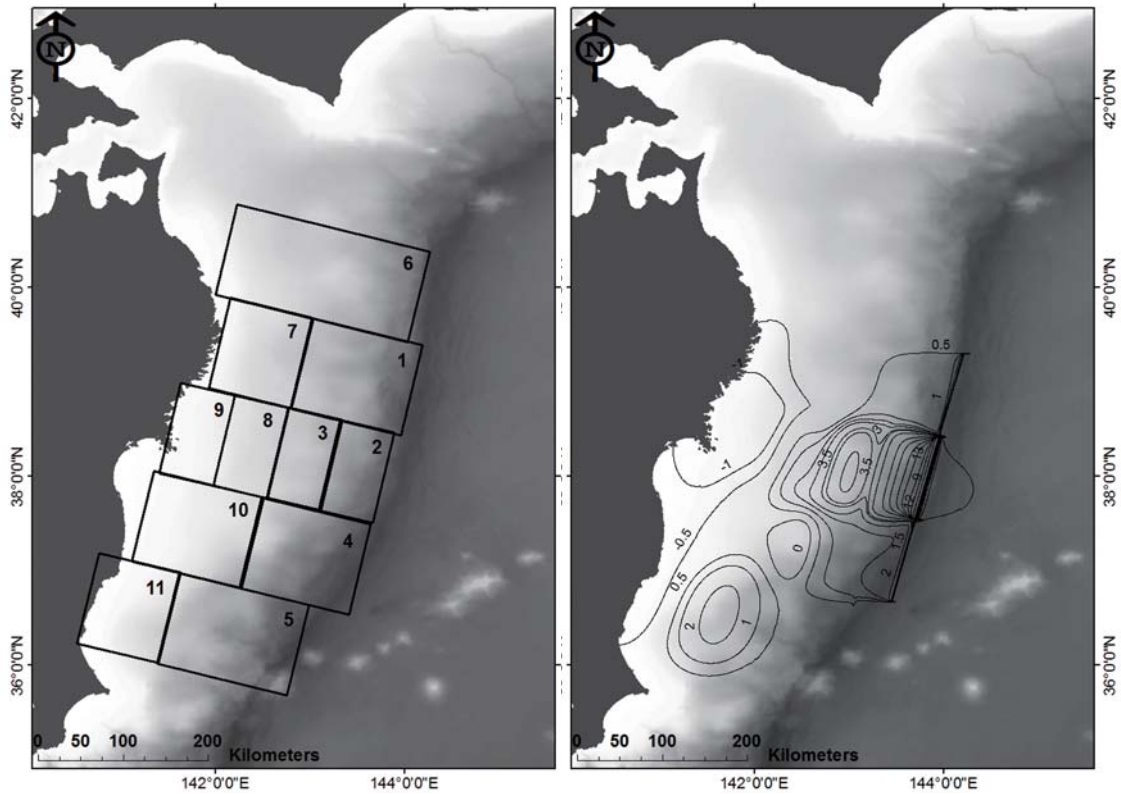
Figure6. Fault segments representing the 2011 rupture area (left), and the resulting calculated sea-floor displacement (right).

better values of K and κ. Only the standard deviation of the amplitude and wave period for the first drop (*a2*) gave values outside the range proposed by Shuto (1991), while the other component in both first peak (*a1*) and first drop (*a2*) produced satisfactory results.

We then moved onto the second validation of the proposed model for the inundation arrival time from the stopped clocks information. As seen in Fig. 7, the results produced by Tohoku Univ. version 1.1 are not so different to those of the present study. Instead, Tohoku Univ. version 1.1 yields a better comparison with the observed data as shown in Table 3. Therefore, we conclude that the only discrepancy from the previous source model is in the modeled tsunami waveforms in the six GPS buoys, which are improved

in this study.

The last validation we present is made using the observed run-up data. The proposed source model produced results overestimated on average 5 m from the observed data (Fig. 8). First the inundation model was performed using a cell size of 90 m, which does not allow a detailed representation of the topography especially in middle Iwate, which has characteristic hilly towns inside a long V-shaped bay. Also, the present inundation model used homogenous bottom friction, which may produce a significantly overestimated result. Muhari et al. (2011) demonstrated that the constant roughness model can produce an inundation parameter double the size of that produced by the spatially distributed roughness model in a densely

Table2. Comparison of Aida numbers in terms of the amplitude and wave period with observational data of six GPS buoys.

Model	Amplitude (m)						Period (min)					
	a1			*a2*			*a1*			*a2*		
	K	*k*	*RMSE*	*K*	*k*	*RMSE*	*K*	*k*	*RMSE*	*K*	*k*	*RMSE*
DCRC	1.2505	1.5359	1.1734	0.2114	1.4738	0.4206	1.1241	1.2658	1.0746	0.3986	3.3711	0.8472
This study	0.9278	1.3181	0.9817	0.9796	2.7003	1.7634	1.0026	1.0580	1.0025	1.4775	2.0693	1.3580
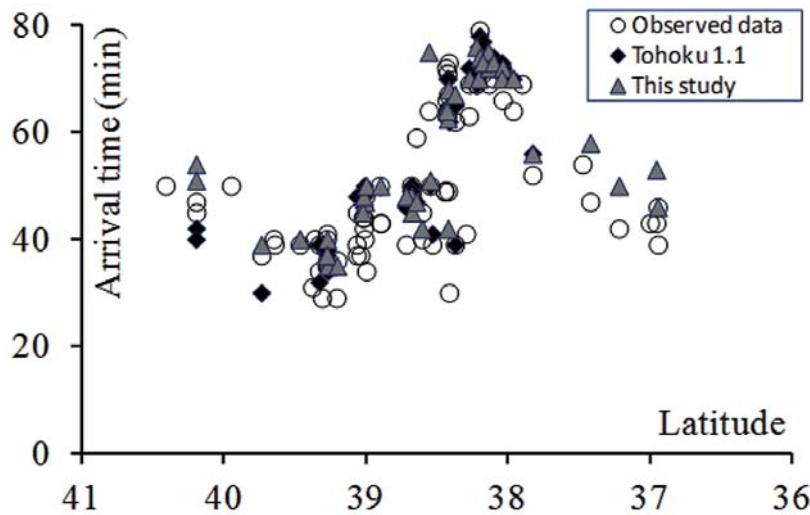
Figure 7 Comparison of the observed and the modeled arrival times based on Tohoku Univ. 1.1 and the present study

Table3. Comparison of the modeled inundation arrival times with the observational data from the stopped clocks

	Tohoku univ. 1.1				This study		
	Initial arrival time	1st Peak amplitude	Range Interval		Initial arrival time	1st Peak amplitude	Range Interval
RMSE	6.791	6.741	5.441	RMSE	11.753	10.381	8.078
% error	7.961	7.285	5.264	% error	16.920	15.075	9.209

populated area. Therefore, we assumed that the present model would produce satisfactory results if used in high accuracy topographic data supported by the accommodation of spatially distributed roughness or resistance due to the existence of buildings. Further study is required to verify the above statement.

4 Characteristics of tsunami arrival time at Sanriku coast during the 2011 East Japan Tsunami

After validating the proposed source model with the observed data, we derived the characteristics of the tsunami arrival time at towns along the Sanriku coast in this section. Definitions in the following explanation are still based on components of arrival time described in Hayashi et al. (2012). We first described the characteristics of the tsunami arrival in north Iwate toward the north up to Oirase town in Aomori Prefecture as given in Fig. 9.

The initial arrival time, local crest and the primary crest in this region are gradually decreased toward the south with values ranging from 16 to 35 min for initial arrival time, 34 to 60 min for local crest and 38 to 68 min for primary crest. This indicates that the
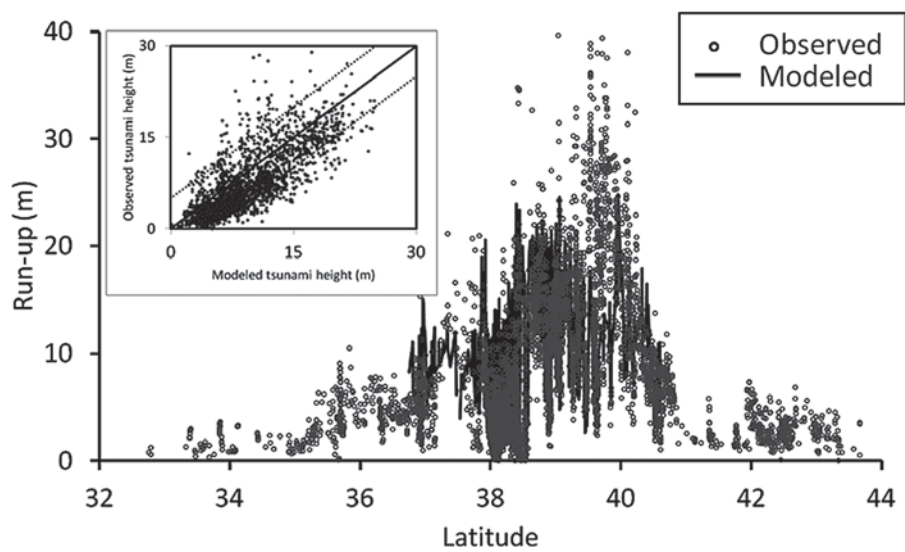

Figure8. Comparison of modeled run-up heights using the proposed source model with the observed data
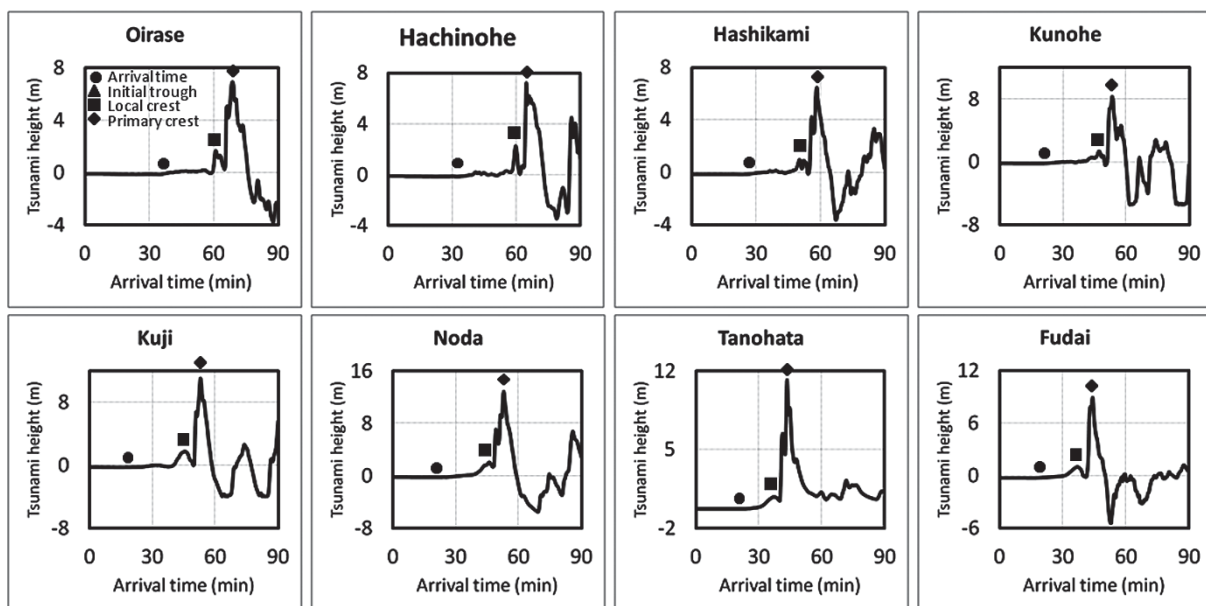

Figure9. Arrival time characteristics from north Iwate to Oirase in Aomori Prefecture

further to the north we go, the further the cities are from the source area. Our numerical results indicate that the local crest exists before the primary types. However, the available tide gauge data before damage by the tsunami do not indicate such information as that of the local crest. Instead, the presumed primary crest was preceded by small receding water (see Hayashi et al., 2011). Nevertheless, the arrival time in Hachinohe and Kuji gave similar results when compared with observed and modeled data; concurrently 30 and 32 min in Hachinohe, and 15 to 22 min in Kuji. A summary of the tsunami arrival in this region is given in Fig. 10.

Moving southward to the region between middle Iwate down to north Miyagi, characteristics of the tsunami arrival time in cities inside the bays on the Sanriku coast can be divided into two categories as given in Fig. 11.
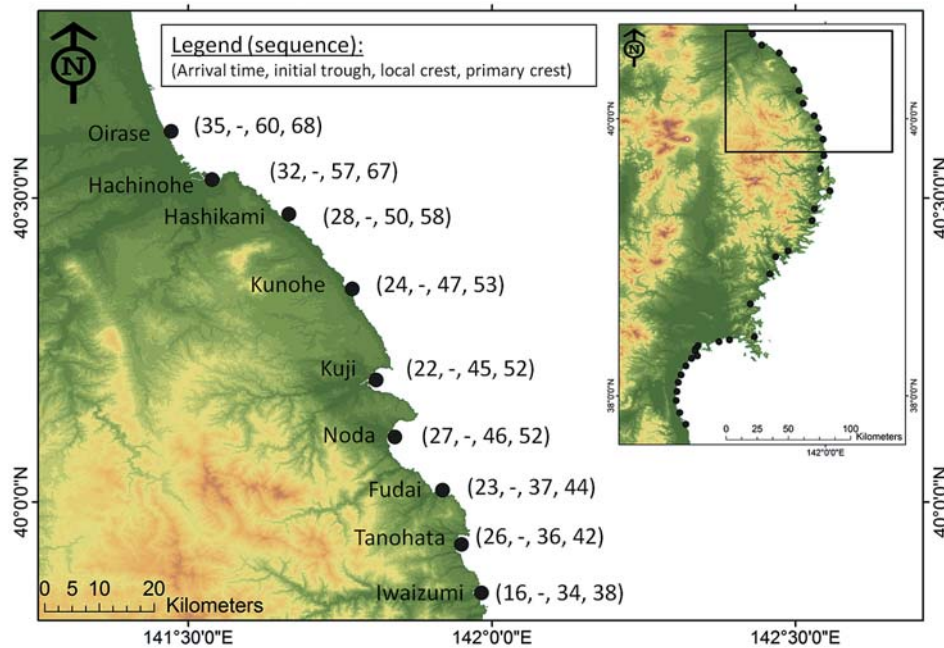

Figure10. Summary of the arrival time characteristics in north Iwate to Aomori
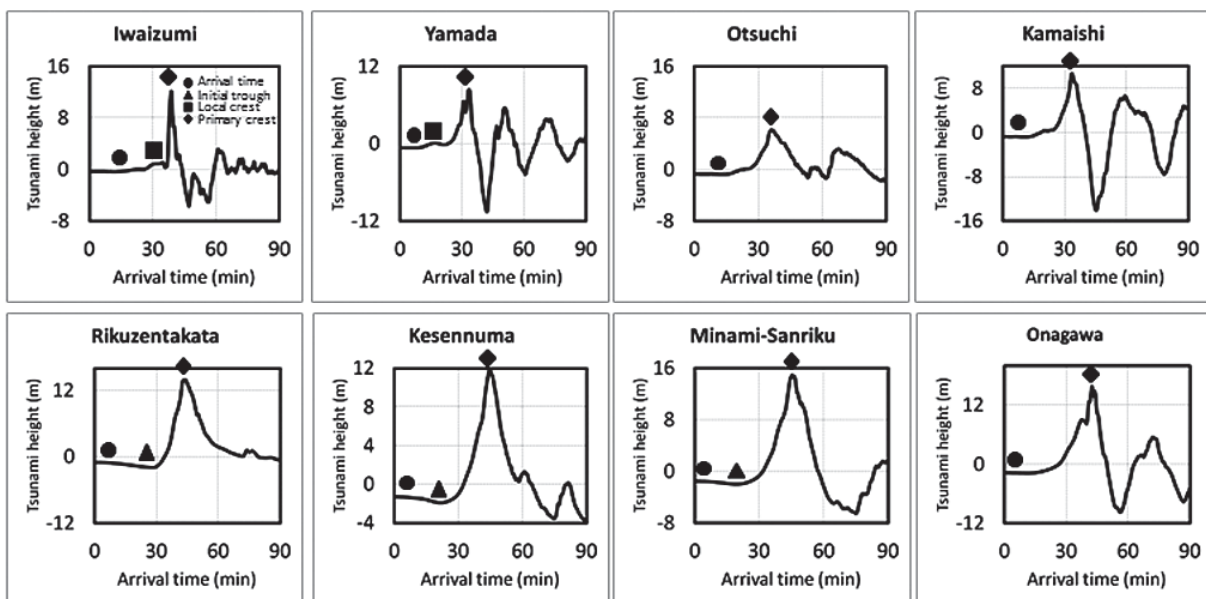

Figure11. Characteristics of tsunami arrival in middle Iwate to the south up to Onagawa town in north Miyagi

First, in Iwate (Iwaizumi down to Kamaishi in the south), the tsunami was not preceded by a leading negative wave (water withdrawal), but a deep receding water came after the first peak. In this area, the influence of the long bay coastal morphology is not significant to delay the arrival time of the tsunami. Here, the primary crest arrives faster than any other area, which ranges from 33 to 36 min. On the contrary, cities in north Miyagi (Rikuzentakata down to Onagawa) experienced short receding water before the first peak arrived. They had negative amplitude after the first peak passed. However, the values are not comparable to the crest's amplitude. In this region, the initial trough is faster toward the south ranging from 10 to 29 min as shown in Fig. 12.

Entering Sendai Bay, all of the cities have similar characteristics of tsunami arrival (Fig. 13). Small receding water precedes the first peak, which comes mostly at 59 to 68 min after the earthquake. Deep receding water is observed after the first peak in Tagajo, Arahama, Natori and Iwanuma.

When compared to the available tide gauge data in Sendai before it was broken by the tsunami (Hayashi et al., 2011), the modeled arrival time and initial trough are close to the observed data with the values of observed and modeled being 5 and 5 min for the arrival time, and 45 to 40 min for initial trough as seen in Fig. 14.
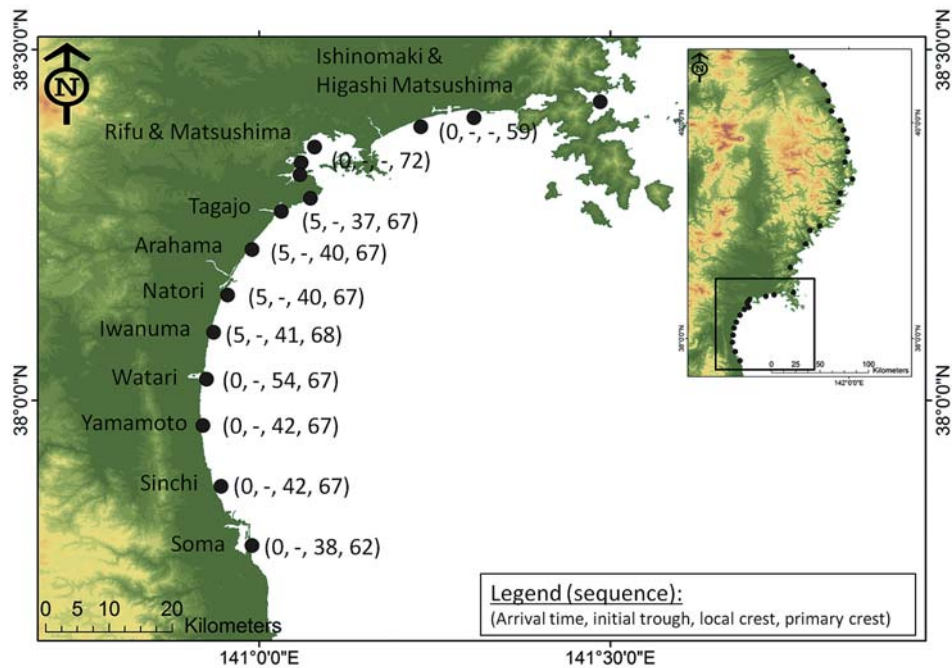
5 Conclusions

We presented and interpreted the arrival time data based on stopped clocks found in the tsunami affected areas and GPS buoys. We demonstrated the
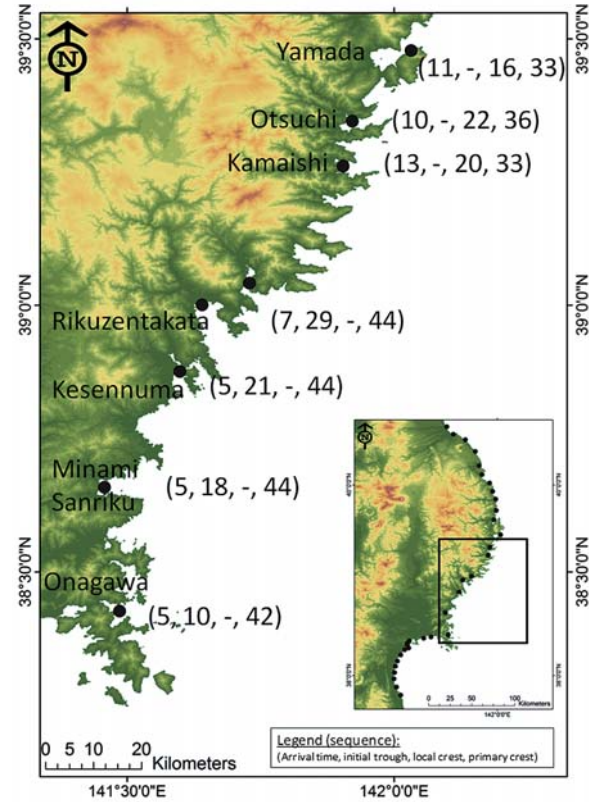
Figure12. Summary of the arrival time in north Miyagi and south Iwate
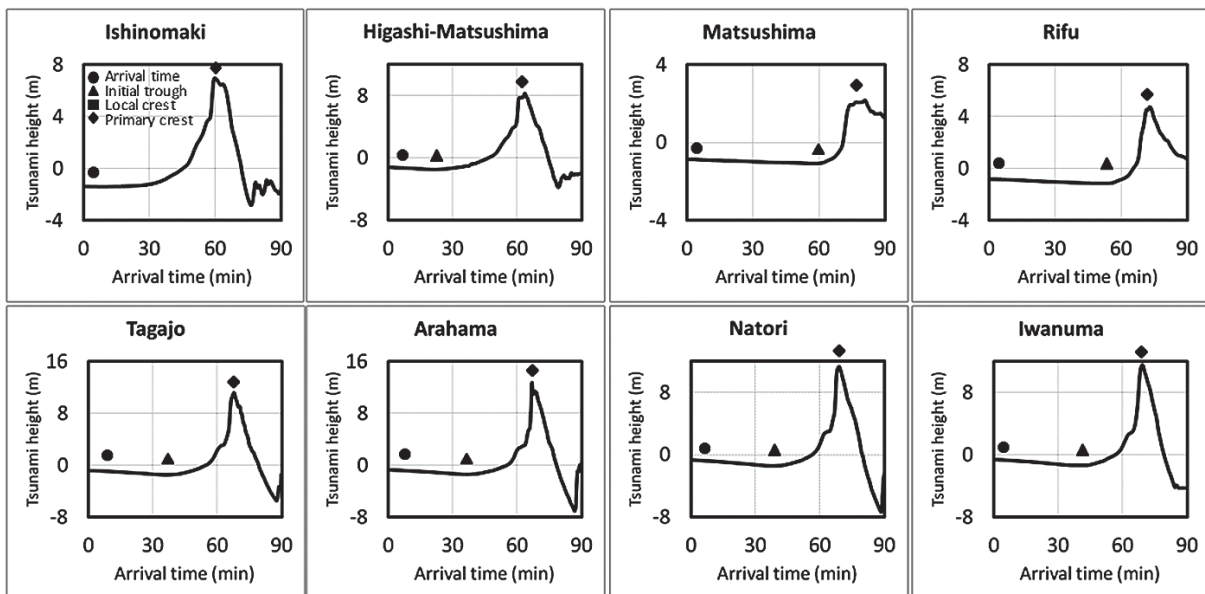
Figure13. Arrival time characteristics in Sendai Plain

101

Figure14. Summary of arrival time in Sendai Plain

use of these data to enhance the tsunami source model based on the available source of Tohoku Univ. version 1.1. Validation of the improved source model gave satisfactory results using the Aida number by taking the arrival time data of GPS, inundation arrival time of stopped clocks and observed run-up height as parameters for validation.

Using the well-validated source model, the tsunami arrival time along the Tohoku coast during the 2011 tsunami was reconstructed. The tsunami arrival time in a specific place is mainly determined by its distance relative to the source (including the effect of the beach's strike relative to the fault's strike) and the shallow sea bottom topography (water depth) that affect the shoaling process. The bay shape coastal morphology has less influence on determining the arrival time. Lastly, through the example of the large tsunami in Japan, we demonstrated that huge tsunamis are not always preceded by a leading negative wave, even for the near-field case.

Acknowledgement

References

Aida, I. (1978), "Reliability of a tsunami source model derived from fault parameters," Journal of Physics of the Earth 26, 57–73.

British Oceanographic Data Centre, The Centenary Edition of the GEBCO Digital Atlas, 2008 (CD-ROM).

Disaster Control Research Center (DCRC), Tohoku University., "Tsunami source model version 1.1, 2011," available at http://www.tsunami.civil.tohoku.ac.jp/hokusai3/J/events/tohoku_2011/model/dcrc_ver1.1_111107.pdf, last accessed 30 March, 2011.

Fujii, Y., Satake, K., Sakai, S., Shinohara, M., Kanazawa, T., "Tsunami source of the 2011 off the Pacific coast of Tohoku earthquake," Earth Planet and Space, Vol. 63 (7), pp 815-820, 2011.

Geist, E. L., & Dmowska, R. (1999), Local Tsunamis and Distributed Slip at the Source. Pure and Applied Geophysics, 154 (3-4), 485-512. doi:10.1007/s000240050241

Geospatial Survey Institute (GSI), "Subsidence investigation due to the earthquake off the coast of the northeastern Pacific Ocean," 2011, available at http://www.gsi.go.jp/sokuchikijun/sokuchikijun40003.html, last accessed 30 March 2011.

Hayashi, Y., Tsushima, H., Hirata, K., Kimura, K., Maeda, K., "Tsunami source area of the 2011 off the Pacific coast of Tohoku earthquake determined from tsunami arrival times at offshore observation station," Earth Planet and Space, Vol. 63 (7), pp 809-813, 2011.

Hoppe, M and Mahadiko, HS. (2010), Thirty Minutes in the city of Padang: Lessons for tsunami preparedness and early warning from the earthquake on September 30, 2009. Working Document no. 25, German-Indonesia Tsunami Early Warning (GI-TEWS), GTZ-IS.

Imamura, F., Review of tsunami simulation with a finite difference method, in: Long wave run-up models, edited by: Yeh, H., Liu, P., and Synolakis, C., World Scientific, Singapore, 25–42, 1996.

Imamura, F., Fujima, K., Arikawa, T., Field survey of the 2010 Chilean tsunami, Report of the Disaster Control Research Center (DCRC), pp 83-89. 2010.

Indonesian Rapid Assessment Team (I-RAPID) (2012), Evaluation of the Indonesian tsunami early warning system on the April 2012 Aceh earthquake. (In Indonesian)

Japan Society of Civil Engineers (JSCE), Tsunami assessment method for nuclear power plants in Japan, The Nuclear Evaluation Sub-Committee, 2002.

Japan Society of Civil Engineers (JSCE), "The 2011 off the Pacific coast of Tohoku earthquake tsunami information," 2011, available at http://www.coastal.jp/ttjt/ last accessed 30 March, 2011.

Lavigne, F., Paris, R., Grancher, D., Wassmer, P., Brunstein, D., Vautier, F., Leone, F., Flohic, F., De Coster, B and Gunawan, T., Reconstruction of tsunami inland propagation on December 26, 2004 in Banda Aceh, Indonesia, through field investigations, Pageoph Topical Volumes, pp 259-281, 2009.

Lay, T., Ammon, C. J., Kanamori, H., Xue, L., & Kim, M. J. (2011), Possible large near-trench slip during the 2011 M w 9.0 off the Pacific coast of Tohoku Earthquake. Earth, Planets and Space, 63(7), 687-692. doi:10.5047/eps.2011.05.033

MacInnes, B T., Gusman AR., LeVeque RJ., Tanioka, Y., Comparison of earthquake source model for the 2011 Tohoku-Oki event using tsunami simulations and near field observations, (in press) available at

http://faculty.washington.edu/rjl/pubs/tohoku1/

Mas, E., Imamura, F., & Koshimura, S. (2012), An Agent Based Model for the Tsunami Evacuation Simulation. A Case Study of the 2011 Great East Japan Tsunami in Arahama Town. Joint Conference Proceeding. 9th International Conference on Urban Earthquake Engineering & 4th Asia Conference on Earthquake Engineering. Tokyo Institute of Technology, Tokyo, Japan.

Maeda, T., Furumura, T., Sakai, S, and Shinohara, M., "Significant tsunami observed at ocean-bottom pressure gauges during the 2011 off the Pacific coast of Tohoku earthquake," Earth Planet and Space, Vol. 63 (7), pp 803-808, 2011.

Ministry of Land, Infrastructures and Transport (MLIT), "The nation-wide ocean wave information network for ports and harbors," 2011, available at http://www.mlit.go.jp/kowan/nowphas/index_eng.html, last access 30 March 2011.

Mori, N., & Takahashi, T. (2012), Nationwide Post Event Survey and Analysis of the 2011 Tohoku Earthquake Tsunami. Coastal Engineering Journal, 54 (01), 1250001-1. doi:10.1142/S0578563412500015

Muhari, A., Imamura, F., Koshimura, S., Post, J., "Examination of three practical run-up models for assessing tsunami impact on highly populated areas," Natural Hazard and Earth System Science, 11, 3107-3123, 2011.

Okada, Y., "Surface deformation due to shear and tensile faults in a half space," Bull. Seismol. Soc. Am., 75, 1135–1154, 1985.

Satake, K., & Kanamori, H. (1991), Use of tsunami waveforms for earthquake source study. Natural Hazards, 4(2-3), 193-208. doi:10.1007/BF00162787

Shuto, N., Numerical simulation of tsunamis – Its present and near future, Natural Hazard (4), pp 171 – 191, 1991.

Shuto, N and Matsutomi, H., Field survey of the 1993 Hokkaido Nansei-Oki earthquake tsunami, Pure and Applied Geophysics, 144 (3/4), pp 649-663, 1995.

Sorensen, J. H. (1991), "When shall we leave? Factors affecting the timing of evacuation departures," International Journal of Mass Emergencies and Disasters, 9(2), 153-165.

Tanioka, Y. and Seno, T., Sediment effect on tsunami generation of the 1896 Sanriku tsunami earthquake, Geophysical Research Letter, 28 (17), pp 3389-3392, 2001.

The CGIAR Consortium for Spatial Information (CGIAR–CSI),

http://srtm.csi.cgiar.org/SELECTION/inputCoord.asp, Last access: August 2010.

Titov, V., Rabinovich, A. B., Mofjeld, H. O., Thomson, R. E., & González, F. I. (2005), The global reach of the 26 December 2004 Sumatra tsunami. Science (New York, N.Y.), 309(5743), 2045-8. doi:10.1126/science.1114576

Tomoyuki, T., Takeyuki, T., Shuto, N., Imamura, F., Ortiz, M., Source model of the 1993 Hokkaido Nansei-Oki earthquake tsunami, PAGEOPH, 144 (3/4), pp 747-767, 1995.

Tsuji, Y., "Earthquake at 9 PM and tsunami at 2 AM," presentation material on the 400 year anniversary of the 1611 Keicho-Sanriku earthquake and tsunami symposium, Tohoku University, 2011a.

Tsuji, Y., Satake, K., Ishibe, T., Harada, T., Kim, H., Nishiyama, A., Murotani, S., Ueno, T., Sugimoto, M., Oki, S., Kusumoto, S., Tomari, J., Heidarzadeh, M., Imai, K., Choi, B., Yoon, S., Bae, J., Kim, K., Characteristics of the height distribution of the tsunami of the 2011 East Japan Earthquake on Sanriku and Kanto coasts. Paper presented at American Geophysical Union, fall meeting 2011b.

Sugawara, D., Imamura, F., Goto, K., Matsumoto, H., & Minoura, K. (2012), The 2011 Tohoku-oki Earthquake Tsunami: Similarities and differences to the 869 Jogan Tsunami on the Sendai Plain. Pure and Applied Geophysics.
doi:10.1007/s00024-012-0460-1.

Yamazaki, Y., Lay, T., Cheung, K. F., Yue, H., & Kanamori, H. (2011), Modeling near-field tsunami observations to improve finite-fault slip models for the 11 March 2011 Tohoku earthquake. Geophysical Research Letters, 38(March), 18-23. doi:10.1029/2011GL049130

Yue, H., & Lay, T. (2011), Inversion of high-rate (1 sps) GPS data for rupture process of the 11 March 2011 Tohoku earthquake (M w 9.1). Geophysical Research Letters, 38(March), 1-6. doi:10.1029/2011GL048700